Dhaka Univ. J. Sci. 58(1): 41-44 2010 (January)

Slope of ΔV–t curves of Evoked Muscle Potentials for Diagnosis of Neural Disorders

M. K. U. Sikder[1] and K. S. Rabbani [2]

Department of Physics, Dhaka University, Dhaka-1000, Bangladesh

Received on 10.08.2008. Accepted for Publication on 06.04.2009

Abstract

A nerve trunk consists of many individual nerve fibers with a specific Distribution of Conduction Velocity (DCV), which may change with neural disorders. A technique was earlier presented in which the time distribution of voltage amplitude deviation (ΔV–t) of evoked muscle responses from two conduction distances was used to extract qualitative information on DCV. This was shown to have some degree of success using simulated compound muscle action potentials for various assumed gross disorders of DCV. In the present work slopes of the earlier ΔV–t curves from simulated potentials, and their ratios were used to identify patterns that may provide further indications of the disorders, increasing confidence in the diagnosis.

1. Introduction

Any nerve trunk (or a nerve bundle) has thousands of individual nerve fibers or axons with a specific Distribution of Conduction Velocity (DCV). An ideal diagnosis of neural disorder would require determining the complete DCV of a nerve trunk, however, no practical method for such DCV determination acceptable for clinical diagnosis exists at present. In an evoked potential study, a nerve trunk is stimulated at one or more points and the resulting Compound Motor Action Potential (CMAP) which is evoked from a connected muscle is studied to obtain information on nerve conduction properties. The time delays associated with the different velocities of axons in the nerve trunk and their respective numbers together contribute towards the shape of the CMAP. Instead of looking for a rigorous solution, our group has been looking for qualitative information on DCV by dividing the whole spectrum of velocities into broad groups such as fast, slow and medium fibres, and studying the shapes of CMAP that are generated due to loss of one or more of these groups of nerve fibres. It is felt that in combination with conventional nerve conduction velocity (NCV) values obtained from the onset of CMAP's, this qualitative information on the shape of CMAP's, leading to some information of DCV, will offer a degree of improvement in the clinical diagnosis. Several techniques are being studied with this aim and some identifying features have already been successfully determined for synthesised CMAP's in our laboratory[1-8].

A CMAP is usually synthesized from motor unit action potentials (MUAP), which is the combined action potential from all muscle fibres, supplied by the branches of a single nerve axon. Since the CMAP is usually bipolar in shape[9-11], it is natural to assume a similar shape for the MUAP, which was done in these earlier works. Though there are various factors that influence the final wave shape of MUAP as well as of CMAP, it has been observed that if relative electrode positions are kept nearly the same with respect to surface anatomy, the waveforms obtained from the same subject at different times and from different subjects have similar shapes if they are free from neurological disorders[1]. For simplicity, in the earlier work[3,7,8] all MUAP's have been assumed to have the same shape and amplitude and all motor units have been assumed to have the same delay at the neuro-muscular junctions. Conduction delays due to distances from muscle fibers to electrodes were also ignored since these delays are very small compared to the conduction delays of the nerve signals. It was also found in our laboratory, that relevant features of a CMAP are relatively insensitive to the shapes of MUAP's used for the synthesis[5]. Based on the above information we used a sinusoidal pattern in our earlier work[7,8], as it is easier to manipulate. The mathematical model of a CMAP having sinusoidal wave shape for one complete period was represented as,

$$C_t = \sum_{i=1}^{N} n_i\, m_{i\,t} \;,\quad i = 1, 2, 3, \ldots N;\ i, t \text{ are integers} \qquad (1)$$

Where, n_i is the number of fibers in the ith group with conduction velocity V_i (the corresponding group action potential being $n_i m_{it}$), and N is the total number of velocity groups and

$$m_{it} = \begin{cases} 0 & \text{for } t < \tau_i; \quad \text{where } \tau_i = \left(\dfrac{d}{V_i} + \tau_0\right) \\ 0 & \text{for } t > \tau_i + T; \quad \text{where } T = 2\pi / \omega \\ -a \sin \omega (t - \tau_i) & \text{otherwise (this forms MUAP waves)} \end{cases} \qquad (2)$$

where, τ_i is the latency from the instant of stimulation to the onset of the MUAP, τ_o is the time delay at neuro-muscular junction, d is the length of the nerve segment, from the point of stimulation to the neuro-muscular junction, T is the time period of each MUAP wave (assumed sinusoidal full wave), and a is its amplitude. A negative sign for the MUAP was used since the first peak of a recorded CMAP is usually negative. For discrete numerical simulation τ_i & T were chosen so that they were all integers (if necessary they were rounded up to the nearest integer value). Based on the above model, the only difference between the different MUAP's were the onset latencies, which arose due to the differences in the velocities of the supplying nerve fibers. This justified the use of CMAP's to extract gross information on DCV's. In our earlier work[8] the CMAP's obtained for two conduction distances were analysed to obtain a ΔV–t curve, where voltage differences between the two curves at different values of time were obtained from the simulated CMAP values. These ΔV–t curves were then compared for several features like amplitude, area under curve, and time spread for pattern recognition purposes. These features, in isolation, or in combination gave some identification tools for the different disorders of DCV, as assumed to start with.

The present work is basically an extension of the above, where some more pattern recognition methods have been

[1] Department of Physics, Jahangirnagar University, Savar, Dhaka 1342
[2] Presently at: Department of Biomedical Physics & Technology, University of Dhaka, Dhaka-1000

used. Here, slopes of simulated ΔV–t curves were obtained and some of the features of these slopes were studied to obtain identification of disorders of DCV.

II. Methods

As in the previous work, four gross cases of nerve degeneration have been assumed for the present work as well, to simulate nerve disorders. These are slow fibre loss (SFL), fast fibre loss (FFL), mid fibre loss (MFL) and a combination of slow and fast fibre losses (SFFL) as indicated in figure 1.

The parameters for simulation work as used in the previous work are reproduced here for ready reference. The nerve fibres were divided into 21 groups with the mean velocities of 40 m/s, 42 m/s, … up to 80 m/s. Number of fibers (n_i) within each group was taken between 400 and 1400 for a normal subject, which was chosen rather arbitrarily in a pattern as shown in Figure 1. For assumed disorders the DCV patterns were changed to represent the gross loss patterns mentioned above and are also shown in the same figure. The values of different parameters as chosen for the simulation were: T = 9 ms, τ_o = 1.5 ms; a was chosen arbitrarily so that the resulting CMAP's have realistic amplitudes. Two conduction distances d_{short} = 0.08 m and d_{long} = 0.24 m were assumed, to correspond to that typically used for measurements on human subjects. CMAPs' were simulated using the mathematical model given above, and from CMAP's corresponding to two conduction distances for the same nerve, ΔV–t curves were obtained.

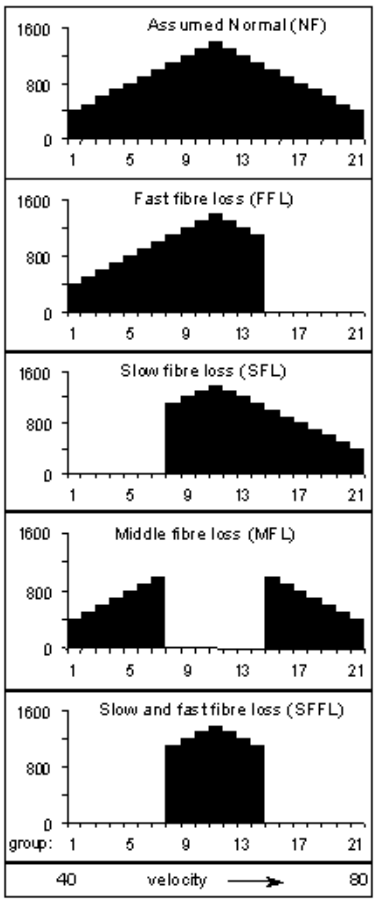

Fig. 1. Assumed DCV to represent electrically stimulated nerve fibers for normal nerve and for different assumed disorders. Vertical axis gives number of fibers.

Slopes of ΔV–t curves

In the present work, the first derivatives (slopes) were obtained from the ΔV–t data obtained in the previous work, for all the types of DCV assumed, to represent normalcy and disorder. Necessary computer algorithm was developed and applied to obtain these slopes of ΔV–t curves as a function of time. All these curves showed four distinct peaks; these are the peak slopes of ΔV–t curves in four segments which we named S_1, S_2, S_3 and S_4 respectively as shown in figure-2, and these were chosen to study the differences between the different disorders. Two ratios of the absolute slopes, $|S_1/S_2|$ and $|S_4/S_3|$ were also computed and studied. In these calculations, final values obtained for different parameters were rounded up to their nearest integers for convenience.

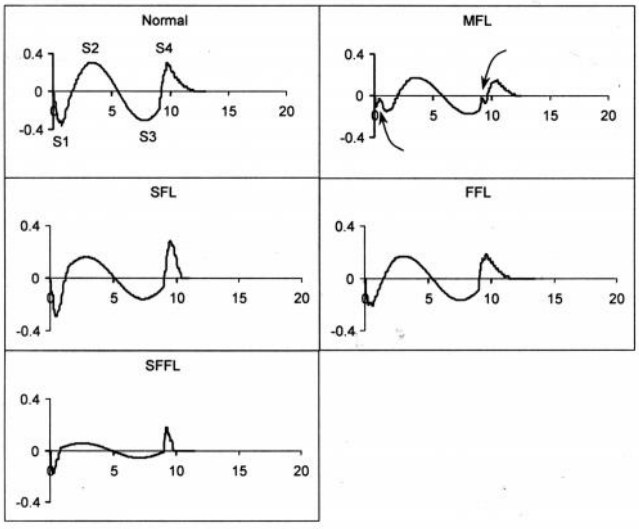

Fig. 2. First derivative of ΔV–t curves for different assumed types of disorders (time in ms along horizontal). Peak values S_1 to S_4 indicated in the top left graph. Note extra peaks for MFL case.

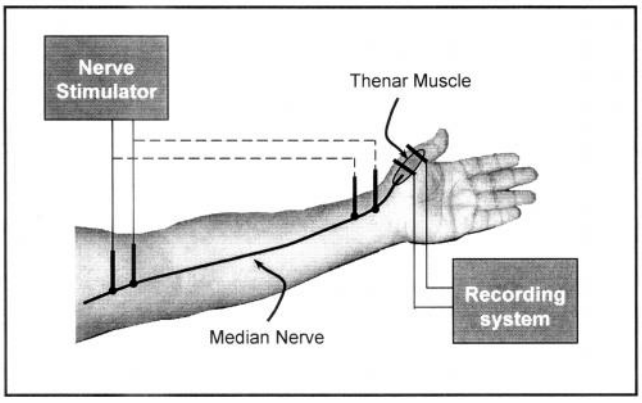

Fig. 3. Block diagram of a measurement system for Combined Muscle Action Potential (CMAP) from a nerve in the hand.

Sensitivity of CMAP matching

The original ΔV–t curve and the derived parameters as used in the present work would depend on the time matching of

the evoked CMAP's for the two conduction distances, which was performed manually (in the earlier work). To see how a slight variation may affect the results, the CMAP response for long conduction distance was shifted in time by about ± 8 % of the total spread (~1 ms in 12 ms). The values and percentage changes obtained in the above features (S_1, S_2, S_3, S_4, $|S_1/S_2|$ and $|S_4/S_3|$) for only two DCV types are given in table 2.

III. Observations and Results

The first derivatives or slopes of ΔV–t curves corresponding to different assumed disorders together with the assumed normal DCV are shown in figure 2. The peaks of these curves are given in table 1. If these peak slopes corresponding to two different DCV's differ significantly these may have the potential to distinguish these DCV's. As can be seen, the values of the slopes S_1, S_2, S_3, S_4, particularly of the ratios, vary significantly between certain DCV types and therefore, may be useful in diagnosis. S_2 and S_3 allow NF and SFFL types to be distinguished within themselves clearly and also allow them to be distinguished from the remaining three types. S_1 and S_4 may allow NF and SFL to be distinguished from FFL, MFL and SFFL types. The ratios in the last two columns may allow distinction of SFFL type clearly, while SFL type may also be distinguished from the rest. NF and FFL are similar in these ratios' but may be distinguished using S_2 and S_3. Therefore the above criteria may be used to identify nerve disorders having the DCV types assumed in this work.

There is one additional feature that can be noticed in figure 2 for the MFL type of DCV. There are two small extra spike-like peaks, one near the beginning and one near the end, which are not present in any of the others. So these extra spikes may be useful in identifying MFL type of DCV from the rest.

In the study for sensitivity to adjustment of the onsets of the two CMAP's, it can be seen that a range of about 0 - 13 % variation is obtained in the parameters of interest for an onset mismatch of 8%. For case of MFL the ratios' of slopes in column 5 and 6 are slightly sensitive but the slopes themselves are relatively insensitive. The differences that were considered significant in the above discussions in order to separate out different types of DCV disorders are of the order of 45% to 200%, as can be seen from the values in this table, and some differences were greater still. Therefore, uncertainties of the order of 10% due to personal errors will not significantly affect the results and the techniques developed in this work are expected to be useful in identifying the DCV patterns, thus improving the diagnosis.

IV. Discussion

In order to diagnose neural disorders, ΔV–t analysis in our previous work presented significant information on different DCV's of nerve fibres based on the variations of amplitude of ΔV–t curve, area under curve and spread in time of CMAP's [8]. In the present work, the value of highest slopes of four segments, S_1, S_2, S_3, S_4 (figure-2), and the ratio's of the absolute slopes $|S_1/S_2|$ and $|S_4/S_3|$ in table 1 show that these values are significantly different for the different assumed nerve disorders. Therefore these parameters would provide additional means for identification of the different types of DCV's. In combination with the earlier results, these would provide a high confidence in the obtained results.

The extra peaks observed for the MFL case in figure 2 is interesting which is not present in the others. Loss of fibres in the middle of the range causes a gap in the MUAP's needed for synthesis of the CMAP. Therefore the occurrence of the extra peak can be explained in view of the above and this provides us with an additional pattern for identification of MFL type DCV.

Table 2 shows that minor differences caused due to personal errors in matching the onsets of the two CMAP's would not affect the identification potential of the methods suggested, as also pointed out in the results section above.

The types of nerve disorders assumed in the present work are not exhaustive, there may be many more. However, the present work, together with the earlier one on ΔV-t analysis offers methods for an improved diagnosis of neural disorders in conjunction with conventional NCV techniques.

Table. 1. Parameters of ΔV–t curves for identification of different disorders

	1	2	3	4	5	6
DCV type	Relative slope, (Min/max)				Ratio of slopes	
	S_1	S_2	S_3	S_4	$\frac{\lvert S_1 \rvert}{\lvert S_2 \rvert}$	$\frac{\lvert S_4 \rvert}{\lvert S_3 \rvert}$
NF	-0.36	0.30	-0.30	0.29	1.2	0.97
SFL	-0.29	0.16	-0.16	0.28	1.87	1.75
FFL	-0.20	0.17	-0.17	0.18	1.18	1.06
MFL	-0.15	0.17	0.17	0.15	0.88	0.88
SFFL	-0.18	0.05	-0.05	0.17	3.60	3.40

Table. 2. Sensitivity of the pattern identifiers to small variations in curve matching

		1	2	3	4	5	6
Nerve DCV types	Time shift of one response	Relative slopes (min/max)				Ratio of slopes	
		S_1	S_2	S_3	S_4	$\frac{\lvert S_1 \rvert}{\lvert S_2 \rvert}$	$\frac{\lvert S_4 \rvert}{\lvert S_3 \rvert}$
NF	+ 1 ms +8 %	-0.360 0%	0.3413 %	-0.3413 %	0.317 %	1.0612 %	0.916 %
	- 1 ms -8 %	-0.32 -11 %	0.26 -13 %	-0.26 -13 %	0.26 -10 %	1.2 0 %	1.00 -3 %
MFL	+ 1 ms +8 %	-0.14 -7 %	0.1912 %	-0.1912 %	0.15 0%	0.74 **16** %	0.79 10 %
	- 1 ms -8 %	-0.16 +7 %	0.15 -12 %	0.15 -12 %	0.15 0%	1.06 **20** %	1.00 **14** %

Annexure

A block diagram of a measurement system for CMAP is given in Fig.3. An electrical nerve stimulator produces pulsed currents which are applied to a nerve trunk running under the skin using electrodes on the surface. This creates action potentials in all the nerve fibres which travel to the linked muscle and create action potentials in each of the muscle fibres in turn. Using electrodes on the skin surface over the muscle, the combined potential, i.e., CMAP, can be sensed, amplified, and acquired using a computer.

---

1. Rabbani K S 1996 Standardization of electro-physiological measurements for numerical investigations in Bangladesh *Research report, Asiatic Society of Bangladesh*
2. Baig T N and K S. Rabbani, 1999 Synthesis of evoked compound nerve action potentials through development of a mathematical model for single fibre action potential, Bangladesh Journal of Science & Technology, Vol.1, p.199-207
3. Baig T N and K S. Rabbani, 2000 Synthesis of evoked compound muscle action potentials through development of a mathematical model and comparison with real observations, Bangladesh Journal of Science & Technology, Vol.2, p.217-224
4. Khan M S I and K S. Rabbani, 2004 Simulated Δt - t distribution of evoked potentials for multiple conduction distances in nerve for diagnosis of neural disorders *Int. Conf on Physics for Understanding and application organised by the Bangladesh Physical Society, Dhaka, Bangladesh.*
5. Islam M N 1996 Simulation of evoked nerve action potentials and their analysis for neurological diagnosis M. Sc. Thesis, *Department of Physics, University of Dhaka, Dhaka*
6. Sabbir S A 1996 M. Sc. thesis, *Department of Computer Science, University of Dhaka, Dhaka*
7. Sikder M K U and K S. Rabbani, 2006 Simulation of evoked muscle action potentials using a simplifying model Dhaka Univ. J. Sci. **54(1)** 105-108
8. Sikder M K U and K S. Rabbani, 2007 ΔV–t analysis of evoked muscle potentials for diagnosis of neural disorders Dhaka Univ. J. Sci. **55(1)** 111-114
9. McGill K C, Z. C. Lateva and S. Xiao, 2001b A model of the muscle action potential for describing the leading edge, terminal wave, and slow afterwave *IEEE Trans. Biomed. Eng.* **48** 1363
10. Lateva Z C, K. C. McGill and C. G. Burgar, 1996 Anatomical and electrophysiological determinants of the human thenar compound muscle action potential *Muscle & Nerve* **19** 1457-68
11. McGill K C and Z. C. Lateva, 2001a A model of the muscle-fibre intracellular action potential waveform, including the slow repolarization phase. *IEEE Trans. Biomed. Eng.* **48** 1483